

Next-to-Leading Order QCD Corrections to the Decay Width $H \rightarrow Z\gamma$

Roberto Bonciani

*Dipartimento di Fisica, Università di Roma “La Sapienza” and INFN Sezione di Roma,
00185 Roma, Italy
E-mail: roberto.bonciani@roma1.infn.it*

Vittorio Del Duca

*Institute for Theoretical Physics, ETH Zurich, 8093 Zurich, Switzerland
and INFN Laboratori Nazionali di Frascati, 00044 Frascati (Roma), Italy
E-mail: delducav@itp.phys.ethz.ch, delduca@lnf.infn.it*

Hjalte Frellesvig

*Institute of Nuclear and Particle Physics, NCSR “Demokritos”,
Agia Paraskevi, 15310, Greece
E-mail: frellesvig@inp.demokritos.gr*

Johannes M. Henn

*Institute for Advanced Study, Princeton, NJ 08540, USA
E-mail: jmhenn@ias.edu*

Francesco Moriello

*Dipartimento di Fisica, Università di Roma “La Sapienza” and INFN Sezione di Roma,
00185 Roma, Italy
E-mail: francesco.moriello@roma1.infn.it*

Vladimir A. Smirnov

*Skobeltsyn Inst. of Nuclear Physics of Moscow State University, 119991 Moscow, Russia
E-mail: smirnov@theory.sinp.msu.ru*

ABSTRACT: We present the analytic calculation of the two-loop QCD corrections to the decay width of a Higgs boson into a photon and a Z boson. The calculation is carried out using integration-by-parts identities for the reduction to master integrals of the scalar integrals, in terms of which we express the amplitude. The calculation of the master integrals is performed using differential equations applied to a set of functions suitably chosen to be of uniform weight. The final result is expressed in terms of logarithms and polylogarithmic functions Li_2 , Li_3 , Li_4 and $\text{Li}_{2,2}$.

KEYWORDS: Higgs decay, Feynman diagrams, Multi-loop calculations.

1. Introduction

The discovery at the Large Hadron Collider (LHC) of the Higgs boson of the Standard Model (SM) [1, 2] calls for the investigation of its properties, with the degree of agreement between the observed and the predicted behaviour being still an open question. The new boson decays into two photons or two electroweak W/Z bosons. It should also decay into a photon and a Z boson. If it is a SM Higgs boson with a mass of 125.1 GeV, the branching ratio is $B(H \rightarrow Z\gamma) = 1.55 \cdot 10^{-3}$, with an uncertainty of about 9% [3]. The $H \rightarrow Z\gamma$ decay is being searched by the CMS [4] and ATLAS [5] Collaborations at the LHC.

The leading order evaluation of the SM $H \rightarrow Z\gamma$ decay was performed long ago [6, 7]. As the Higgs boson has no electric charge, it does not couple directly to photons. Then the decay of a Higgs boson into a photon and a Z boson must be mediated at loop level by charged particles. At one loop, it is mediated by a heavy-quark loop [6] or a W -boson loop [7], just as for the $H \rightarrow \gamma\gamma$ decay. $H \rightarrow Z\gamma$ may provide information on new physics, as a different $H \rightarrow Z\gamma$ decay rate is expected if H is a non-SM scalar boson [8, 9], or a composite state [10], or if different particles circulate in the loop [11, 12, 13].

The two-loop QCD corrections to the $H \rightarrow Z\gamma$ decay were computed numerically in Ref. [14]. They correspond to two-loop corrections generated by a gluonic exchange within the heavy-quark loop. In this paper, we present an analytic calculation of the QCD corrections to $H \rightarrow Z\gamma$.

The paper is organised as follows: in Sect. 2, we recall the definition and the explicit expressions of the amplitude for the decay $H \rightarrow Z\gamma$ at leading order; in Sect. 3, we describe how we perform the analytic computation of the NLO QCD corrections to the decay width; in Sect. 4, we provide numerical results as a function of the Higgs mass; in Sect. 5, we draw our conclusions. The appendices contain details on the projection operators used to define the decay amplitude (App. A), the master integrals (App. B), the matrices of the system of differential equations for the master integrals (App. C) and the analytic properties of the functions occurring in the master integrals (App. D).

2. $H \rightarrow Z\gamma$ at Leading Order

2.1 The amplitude for the decay $H \rightarrow Z\gamma$

At leading order the SM Higgs boson decays into a photon and a Z boson via either a heavy-fermion loop or a W -boson loop. The corresponding Feynman diagrams are shown in Fig. 1. Let us label the Z -boson momentum as p_1 and the photon momentum as p_2 . The general Lorentz structure $T^{\mu\nu}$ of the amplitude,

$$\mathcal{M} = T^{\mu\nu} \varepsilon_\mu(p_1) \varepsilon_\nu(p_2), \quad (2.1)$$

for the decay of a Higgs boson into a Z boson and a photon with polarization vectors $\varepsilon_\mu(p_1)$ and $\varepsilon_\nu(p_2)$ respectively, is

$$T^{\mu\nu} = p_1^\mu p_1^\nu T_1 + p_2^\mu p_2^\nu T_2 + p_1^\mu p_2^\nu T_3 + p_2^\mu p_1^\nu T_4 + \delta^{\mu\nu} T_5 + \epsilon^{\mu\nu\rho\sigma} p_{1\rho} p_{2\sigma} T_6, \quad (2.2)$$

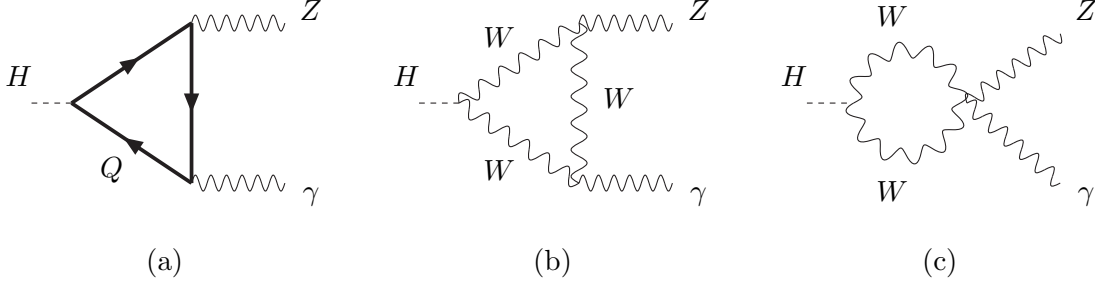


Figure 1: Feynman diagrams for the decay process $H \rightarrow Z\gamma$ at leading order.

where $p^2 = \sum_{i=1}^3 p_i^2 - p_0^2$ and $p_1^2 = -m_Z^2$, $p_2^2 = 0$, $(p_1 + p_2)^2 = -m_H^2$. m_H is the Higgs mass and m_Z is the Z -boson mass. The coefficients T_i are functions of the Mandelstam invariants of the problem under consideration and can be extracted using projector operators $P_i^{\mu\nu}$ such that $T_i = P_{i\mu\nu} T^{\mu\nu}$. The projector operators are collected in Appendix A.

Requiring the photon gauge invariance, $T^{\mu\nu} p_{2\nu} = 0$, in Eq. (2.2), we obtain

$$\begin{aligned} T_1 &= 0, \\ T_5 &= -p_1 \cdot p_2 T_4 = \frac{m_H^2 - m_Z^2}{2} T_4. \end{aligned} \quad (2.3)$$

Furthermore, T_2 , T_3 and T_6^* do not contribute to the squared amplitude $|\mathcal{M}|^2$. Thus, up to contributions which vanish in $|\mathcal{M}|^2$, the form factor $T^{\mu\nu}$ can be written as,

$$T^{\mu\nu} = (p_2^\mu p_1^\nu - p_1 \cdot p_2 \delta^{\mu\nu}) T_4. \quad (2.4)$$

2.2 Leading Order Contribution

The width for the decay of a Higgs boson into a photon and a Z boson can be cast in the following form,

$$\Gamma_{H \rightarrow Z\gamma} = \frac{G_F \alpha^2}{64\sqrt{2}\pi^3 m_H} \frac{(m_H^2 - m_Z^2)^3}{m_H^2} |\mathcal{F}|^2, \quad (2.5)$$

where α is the fine structure constant, G_F is the Fermi constant and where we introduced the function \mathcal{F} related to the form factor T_4 by the following equation,

$$\mathcal{F} = \frac{16\pi^2 m_W}{g^3 s_W^2} T_4. \quad (2.6)$$

In Eq. (2.6), g is the weak coupling constant, $s_W = \sin \theta_W$ is the sine of the weak mixing angle, and m_W is the W -boson mass.

*Note that T_6 receives contribution only from the axial-vector part of the $ZQ\bar{Q}$ vertex. However, since the Higgs particle is a C-even state, and the photon is C-odd, only the C-odd coupling of the Z (*i.e.* the vector coupling and not the axial-vector one) contributes to the decay width. This implies that T_6 does not contribute to the general form factor (2.2). In fact, when we add together the diagrams with an opposite flow of the fermionic arrow, the contribution to T_6 changes in sign, in such a way that in the sum $T_6 = 0$.

The function \mathcal{F} can be expanded in powers of the coupling constants, starting with the one-loop contribution. At leading order we have,

$$\mathcal{F}^{(1l)} = \frac{c_W}{s_W} \mathcal{F}_W^{(1l)} + N_c Q_q \frac{\left(\frac{T_q^3}{2} - Q_q s_W^2\right)}{s_W c_W} \mathcal{F}_q^{(1l)}, \quad (2.7)$$

where N_c is the number of colors, $q = t, b$ labels the type of heavy quark, either a top or a bottom, circulating in the loop, Q_q is the heavy-quark electric charge in units of e , T_q^3 is the third component of the heavy-quark isospin, and $c_W = \cos \theta_W$ is the cosine of the weak mixing angle. The actual expressions for $\mathcal{F}_W^{(1l)}$ and $\mathcal{F}_q^{(1l)}$ are,

$$\begin{aligned} \mathcal{F}_W^{(1l)} = & \frac{(m_H^2 m_Z^2 + 2m_Z^2 m_W^2 - 2m_H^2 m_W^2 - 12m_W^4)}{m_W^2 (m_H^2 - m_Z^2)} \\ & + \frac{(2m_H^2 m_Z^2 m_W^2 - 2m_Z^4 m_W^2 - m_Z^2 m_H^2 - 12m_Z^2 m_W^4)}{m_H^2 (m_H^2 - m_Z^2)^2} I(x_W, y_W) \\ & + \frac{(4m_Z^4 - 2m_Z^2 m_H^2 + 12m_W^2 m_H^2 - 12m_W^2 m_Z^2 - 24m_W^4)}{(m_H^2 - m_Z^2)^2} J(x_W, y_W), \end{aligned} \quad (2.8)$$

$$\mathcal{F}_q^{(1l)} = \frac{8m_q^2}{(m_H^2 - m_Z^2)} + \frac{8m_q^2 m_Z^2}{(m_H^2 - m_Z^2)^2} I(x_q, y_q) + \frac{4m_q^2 (4m_q^2 - m_H^2 + m_Z^2)}{(m_H^2 - m_Z^2)^2} J(x_q, y_q), \quad (2.9)$$

with

$$I(x_f, y_f) = \sqrt{1 - \frac{4m_f^2}{m_H^2}} \log(x_f) - \sqrt{1 - \frac{4m_f^2}{m_H^2}} \log(y_f), \quad (2.10)$$

$$J(x_f, y_f) = \frac{1}{2} \log^2(x_f) - \frac{1}{2} \log^2(y_f), \quad (2.11)$$

where the variables x_f and y_f are defined through,

$$m_H^2 = -m_f^2 \frac{(1 - x_f)^2}{x_f}, \quad m_Z^2 = -m_f^2 \frac{(1 - y_f)^2}{y_f}, \quad (2.12)$$

with $f = W, q$ and $q = t, b$.

Let us consider real values of m_t , m_W , m_Z and m_H . In the region $0 < m_H < 2m_f$, x_f has an imaginary part, with unit modulus and phase between 0 and π ,

$$x_f = \exp \left\{ i \arctan \frac{\sqrt{m_H^2 (4m_f^2 - m_H^2)}}{2m_f^2 - m_H^2} \right\}. \quad (2.13)$$

In the region $m_H > 2m_f$, we have $-1 < x_f < 0$; we define $x_f = -x'_f + i0$ with

$$x'_f = \frac{\sqrt{m_H^2} - \sqrt{m_H^2 - 4m_f^2}}{\sqrt{m_H^2} + \sqrt{m_H^2 - 4m_f^2}}. \quad (2.14)$$

Analogously, in the case $0 < m_Z < 2m_f$ the variables y_f are on the unit circle

$$y_f = \exp \left\{ i \arctan \frac{\sqrt{m_Z^2 (4m_f^2 - m_Z^2)}}{2m_f^2 - m_Z^2} \right\}, \quad (2.15)$$

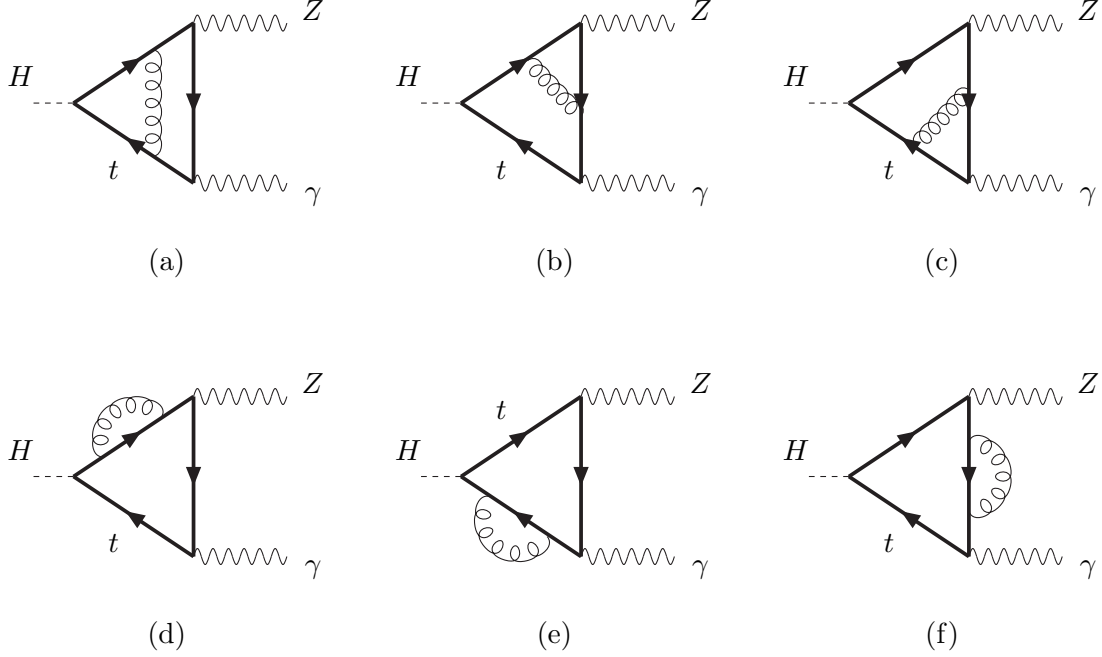


Figure 2: Feynman diagrams for the NLO QCD corrections to the decay process $H \rightarrow Z\gamma$. Diagrams with the reversed direction of the fermionic arrow are not shown. We can easily consider the N_h^2 contribution (one top-quark loop coupled to the Higgs and the other correcting the Z or γ propagator).

while for $m_Z > 2m_f$ we define $y_f = -y'_f + i0$ with

$$y'_f = \frac{\sqrt{m_Z^2} - \sqrt{m_Z^2 - 4m_f^2}}{\sqrt{m_Z^2} + \sqrt{m_Z^2 - 4m_f^2}}. \quad (2.16)$$

3. NLO QCD Corrections

The diagrams involved in the calculation of the NLO QCD corrections to the decay width of a Higgs boson into a photon and a Z boson are shown in Fig. 2. Their contribution to the form factors can be extracted using the projectors defined in Appendix A. Expanding in the strong coupling constant we have,

$$\mathcal{F} = \mathcal{F}^{(1l)} + \frac{\alpha_S}{\pi} \mathcal{F}_0^{(2l)} + \dots, \quad (3.1)$$

At this order in α_S , the bare form factor, $\mathcal{F}_0^{(2l)}$, is UV divergent and needs to be renormalized. The only renormalization required is the heavy-quark mass renormalization, in the fermionic propagators and in the coupling of the Higgs boson to the heavy-quark pair. We choose to perform the mass renormalization in the on-shell (OS) scheme [15],

$$\delta m_{OS}^{(1l)}\left(\epsilon, m_q, \frac{\mu^2}{m_q^2}\right) = -m_q \frac{\alpha_S}{\pi} C(\epsilon) \left(\frac{\mu^2}{m_q^2}\right)^\epsilon \frac{C_F}{4} \frac{(3-2\epsilon)}{\epsilon(1-2\epsilon)}, \quad (3.2)$$

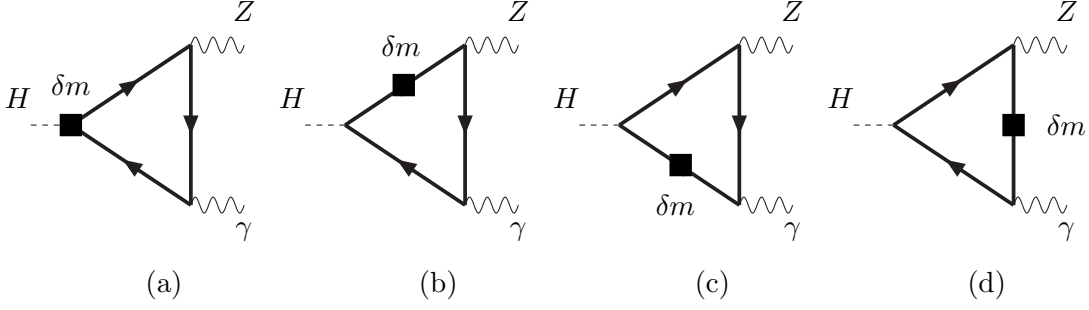


Figure 3: Counterterm diagrams involved in the heavy-quark mass renormalization.

where μ is the renormalization scale, $C_F = (N_c^2 - 1)/(2N_c)$ with N_c the number of colors, $C(\epsilon) = (4\pi)^\epsilon \Gamma(1 + \epsilon)$ and $\epsilon = (4 - d)/2$, with d the space-time dimension. Indicating with $\mathcal{F}^{(2l)}$ the renormalized form factor, we have

$$\mathcal{F}^{(2l)} = \mathcal{F}_0^{(2l)} + \delta m_{OS}^{(1l)} CT. \quad (3.3)$$

The contributions to the counterterm come from the diagrams shown in Fig. 3.

Retaining only terms of $\mathcal{O}(\alpha_S)$, Eq. (2.5) can be written as,

$$\begin{aligned} \Gamma_{H \rightarrow Z\gamma} &= \frac{G_\mu \alpha^2}{64\sqrt{2}\pi^3 m_H} \frac{(m_H^2 - m_Z^2)^3}{m_H^2} \left\{ \Re(\mathcal{F}^{(1l)})^2 + \Im(\mathcal{F}^{(1l)})^2 \right. \\ &\quad \left. + 2 \frac{\alpha_S}{\pi} \left[\Re(\mathcal{F}^{(1l)})\Re(\mathcal{F}^{(2l)}) + \Im(\mathcal{F}^{(1l)})\Im(\mathcal{F}^{(2l)}) \right] \right\} \\ &= \Gamma_{H \rightarrow Z\gamma}^{(1l)} (1 + \delta_{QCD}), \end{aligned} \quad (3.4)$$

where we defined

$$\delta_{QCD} = 2 \frac{\alpha_S}{\pi} \frac{\Re(\mathcal{F}^{(1l)})\Re(\mathcal{F}^{(2l)}) + \Im(\mathcal{F}^{(1l)})\Im(\mathcal{F}^{(2l)})}{\Re(\mathcal{F}^{(1l)})^2 + \Im(\mathcal{F}^{(1l)})^2} \quad (3.5)$$

as of the NLO QCD corrections with respect to the LO contribution.

3.1 Calculation of the master integrals

$\mathcal{F}^{(2l)}$ is expressed in terms of a large number of scalar integrals that are individually ultra-violet divergent. To deal with these divergences, we perform the integrals in dimensional regularization [16, 17, 18, 19, 20, 21]. The dimensionally regularized scalar integrals are not all independent. The reduction to a set of independent integrals, called master integrals, is carried out using two different computer programs, FIRE [22, 23, 24] and Reduze [25, 26], that implement in an automatic way the solution of the linear system of integration-by-parts identities [27, 28] which relate the Feynman integrals.

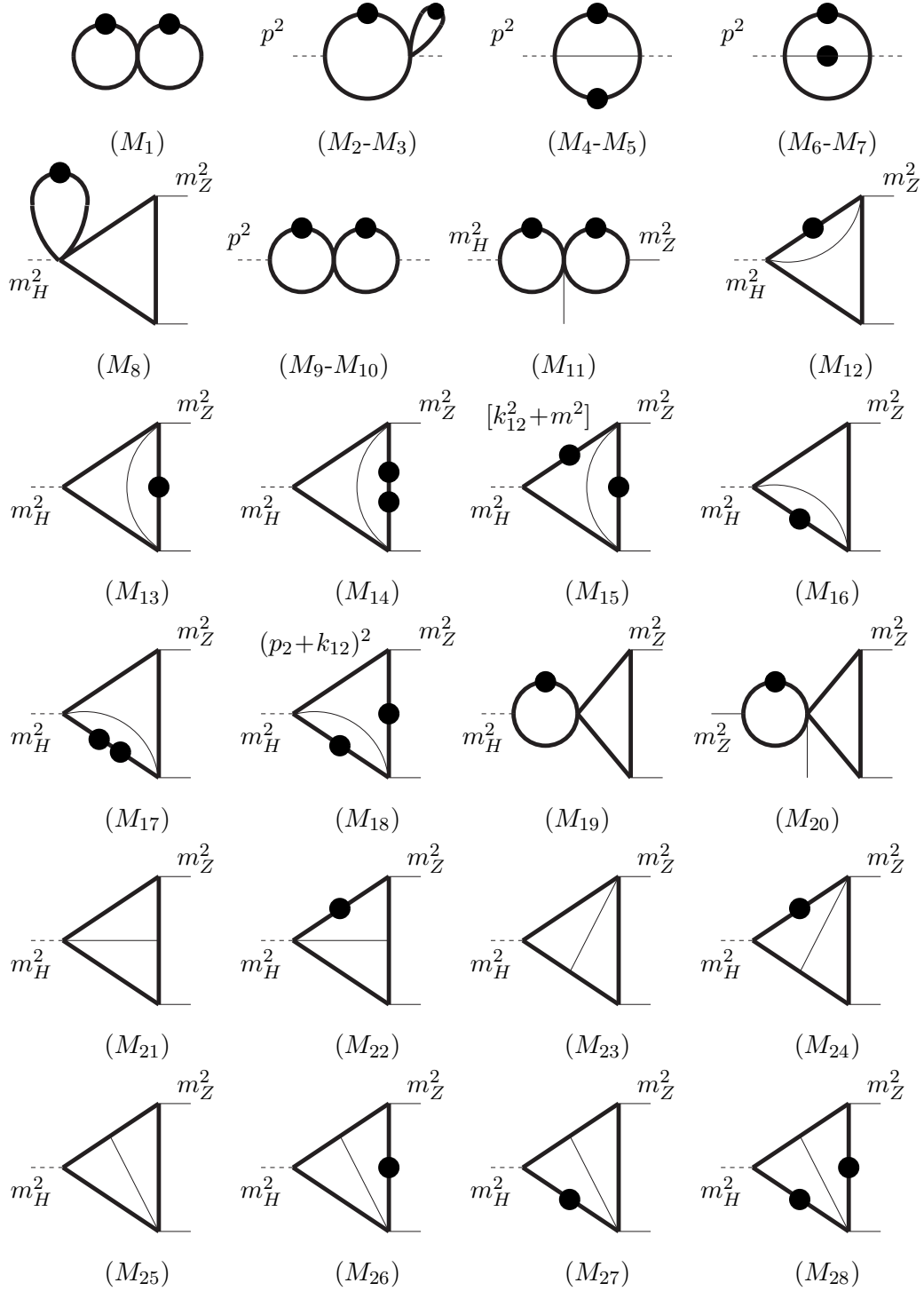


Figure 4: Set of master integrals for the NLO QCD corrections to the decay $H \rightarrow Z\gamma$. The master integrals M_2 , M_4 , M_6 , M_9 are functions of $p^2 = -m_H^2$, while the master integrals M_3 , M_5 , M_7 , M_{10} are functions of $p^2 = -m_Z^2$. M_{15} and M_{18} have the numerator explicitly written. A dot on a propagator indicates that the propagator is raised to power 2. Two dots means that the propagator is raised to power 3. See Appendix B.

We calculate the master integrals using the Differential Equations Method [29, 30, 31, 32, 33, 34, 35], following recent developments [36, 37, 38, 39, 40] (see also [41, 42, 43, 44, 45, 46] and [47, 48] for further studies of the method).

The system of linear differential equations is cast, via a suitable basis choice for the master integrals, in the canonical form [36],

$$d\mathbf{f} = \epsilon d\tilde{A} \mathbf{f} . \quad (3.6)$$

The ϵ dependence is completely factorized from the matrix $d\tilde{A}$. The latter depends only on the dimensionless variables x_q and y_q , defined in Eq. (2.12).

\mathbf{f} is a vector of 28 functions, $f_i(x_q, y_q, \epsilon)$, defined in terms of the integrals drawn in Fig. 4,

$$f_1 = 16 \epsilon^2 M_1 , \quad (3.7)$$

$$f_2 = 16 \epsilon^2 m_H^2 M_{14} , \quad (3.8)$$

$$f_3 = 8 \epsilon^2 \sqrt{-m_H^2(4m_q^2 - m_H^2)} (M_4 + 2M_6) , \quad (3.9)$$

$$f_4 = 16 \epsilon^2 m_Z^2 M_5 , \quad (3.10)$$

$$f_5 = 8 \epsilon^2 \sqrt{-m_Z^2(4m_q^2 - m_Z^2)} (M_5 + 2M_7) , \quad (3.11)$$

$$f_6 = 16 \epsilon^2 \sqrt{-m_Z^2(4m_q^2 - m_Z^2)} M_3 , \quad (3.12)$$

$$f_7 = 16 \epsilon^2 \sqrt{-m_H^2(4m_q^2 - m_H^2)} M_2 , \quad (3.13)$$

$$f_8 = 16 \epsilon^3 (m_H^2 - m_Z^2) M_{16} , \quad (3.14)$$

$$f_9 = 16 \epsilon^2 m_q^2 (m_H^2 - m_Z^2) M_{17} , \quad (3.15)$$

$$f_{10} = 4\epsilon^2 \sqrt{1 - \frac{4m_q^2}{m_Z^2}} \left[m_H^2 (4m_q^2 M_{17} - M_4) + 4m_Z^2 (m_q^2 M_{17} - M_{18}) \right. \\ \left. - 2\epsilon (m_H^2 + m_Z^2) M_{16} \right] , \quad (3.16)$$

$$f_{11} = 16 \epsilon^3 (m_H^2 - m_Z^2) M_{13} , \quad (3.17)$$

$$f_{12} = 16 \epsilon^2 m_q^2 (m_H^2 - m_Z^2) M_{14} , \quad (3.18)$$

$$f_{13} = 4\epsilon^2 \frac{1}{2m_q^2 - m_H^2} \sqrt{1 - \frac{4m_q^2}{m_H^2}} \left\{ m_Z^2 \frac{4m_q^2 m_H^2 - m_H^2 m_Z^2 + m_Z^4}{m_H^2 - m_Z^2} M_5 \right. \\ \left. - 4m_H^2 \frac{m_q^2 m_H^2 - m_H^2 m_Z^2 + m_Z^4}{m_H^2 - m_Z^2} M_{15} - 4m_q^2 (m_H^2 - m_Z^2) m_Z^2 M_{14} \right. \\ \left. + 2\epsilon (2m_q^2 m_H^2 + m_H^2 m_Z^2 - m_Z^4) M_{13} \right\} , \quad (3.19)$$

$$f_{14} = 16 \epsilon^3 (m_H^2 - m_Z^2) M_{12} , \quad (3.20)$$

$$f_{15} = 16 \epsilon^2 m_Z^2 (4m_q^2 - m_Z^2) M_{10} , \quad (3.21)$$

$$f_{16} = 16 \epsilon^2 \sqrt{-m_H^2(4m_q^2 - m_H^2)} \sqrt{-m_Z^2(4m_q^2 - m_Z^2)} M_{11} , \quad (3.22)$$

$$f_{17} = 16 \epsilon^3 (m_H^2 - m_Z^2) \sqrt{-m_Z^2(4m_q^2 - m_Z^2)} M_{20} , \quad (3.23)$$

$$f_{18} = 16 \epsilon^4 (m_H^2 - m_Z^2) M_{21}, \quad (3.24)$$

$$f_{19} = 16 \epsilon^3 (m_H^2 - m_Z^2) \sqrt{-m_Z^2(4m_q^2 - m_Z^2)} M_{22}, \quad (3.25)$$

$$f_{20} = 16 \epsilon^4 (m_H^2 - m_Z^2) M_{25}, \quad (3.26)$$

$$f_{21} = -16 \epsilon^3 m_Z^2 (m_H^2 - m_Z^2) \sqrt{-m_Z^2(4m_q^2 - m_Z^2)} M_{26}, \quad (3.27)$$

$$f_{22} = 16 \epsilon^3 (m_H^2 - m_Z^2) \sqrt{-m_H^2(4m_q^2 - m_H^2)} M_{27}, \quad (3.28)$$

$$f_{23} = 16 \epsilon^2 [2(m_H^2 m_Z^2 - 2m_q^2 m_H^2 - 2m_q^2 m_Z^2) M_{11} + m_q^2 (m_H^2 - m_Z^2)^2 M_{28} \\ + \epsilon(m_H^2 - m_Z^2)(m_Z^2 M_{26} - m_H^2 M_{27})], \quad (3.29)$$

$$f_{24} = 16 \epsilon^4 (m_H^2 - m_Z^2) M_{23}, \quad (3.30)$$

$$f_{25} = 16 \epsilon^3 (m_H^2 - m_Z^2) \sqrt{-m_H^2(4m_q^2 - m_H^2)} M_{24}, \quad (3.31)$$

$$f_{26} = 16 \epsilon^3 (m_H^2 - m_Z^2) M_8, \quad (3.32)$$

$$f_{27} = 16 \epsilon^2 m_H^2 (4m_q^2 - m_H^2) M_9, \quad (3.33)$$

$$f_{28} = 16 \epsilon^3 (m_H^2 - m_Z^2) \sqrt{-m_H^2(4m_q^2 - m_H^2)} M_{19}. \quad (3.34)$$

The functions $f_i(x_q, y_q, \epsilon)$ are chosen in such a way to be pure and of uniform weight, in the sense of [36].

The explicit definition of the integrals M_1, \dots, M_{28} is given in Appendix B[†]. To set the normalization, we define M_1 as the following integral,

$$M_1 = \int \mathcal{D}^D k_1 \mathcal{D}^D k_2 \frac{1}{(k_1^2 + m_q^2)^2} \frac{1}{(k_2^2 + m_q^2)^2} = \frac{1}{16\epsilon^2}, \quad (3.35)$$

where the integration measure is such that,

$$d^D k_1 = 4\pi^{2-\epsilon} \Gamma(1+\epsilon) \left(\frac{\mu^2}{m_q^2} \right)^\epsilon \mathcal{D}^D k_1. \quad (3.36)$$

With this normalization,

$$f_1 = 1. \quad (3.37)$$

The matrix $d\tilde{A}$ is a differential depending on x_q and y_q ,

$$d\tilde{A} = \mathbb{S}_1 d \log x_q + \mathbb{S}_2 d \log (1 - x_q) + \mathbb{S}_3 d \log (1 + x_q) + \mathbb{S}_4 d \log y_q + \mathbb{S}_5 d \log (1 - y_q) \\ + \mathbb{S}_6 d \log (1 + y_q) + \mathbb{S}_7 d \log (x_q - y_q) + \mathbb{S}_8 d \log (1 - x_q y_q) \\ + \mathbb{S}_9 d \log (1 - x_q - x_q y_q + x_q^2) + \mathbb{S}_{10} d \log (1 - y_q - x_q y_q + y_q^2) \\ + \mathbb{S}_{11} d \log (x_q - y_q + x_q y_q - x_q^2 y_q) + \mathbb{S}_{12} d \log (x_q - y_q - x_q y_q + x_q y_q^2). \quad (3.38)$$

The sparse matrices \mathbb{S}_i are purely numerical and they are collected in Appendix C.

To fully describe the \mathbf{f} , we need to complement the differential equations with boundary conditions. We can, in principle, choose any kinematic point (x_q, y_q) . However, it is well known that often, (spurious) singularities of the differential equations allow one to fix the

[†]The calculation of some of the master integrals in Fig. 4 was already performed in Ref. [49].

boundary condition without calculation, using the physical insight that certain limits must be non-singular. This is also the case here. We notice that the integrals defining the primary basis (Fig. 4) are regular in the point $s = m_Z^2 = 0$. Moreover the rational prefactors of the combinations given in Eqs. (3.7–3.34) vanish in the same limit. Therefore, all the integrals $f_i(x_q, y_q)$, $i = 2, \dots, 28$, vanish in this limit. The only exception is represented by f_1 , which is identically equal to 1. We can write the full set of boundary conditions in the compact form,

$$f_i(1, 1) = \delta_{1,i}. \quad (3.39)$$

The system (3.6), together with the boundary condition (3.39), makes it obvious that the solution, i.e. the functions $f_i(x_q, y_q)$, have a number of desirable properties. At any order in the expansion in ϵ , they are given by iterated integrals [50] over the one-form $d\tilde{A}$. Defining the weight of an iterated integral as the number of integrations, we see that at order ϵ^k , \mathbf{f} is given by a \mathbb{Q} -linear combination of iterated integrals of weight k . Such functions are referred to as pure functions of uniform weight.

The basis choice for \mathbf{f} leading to this form was achieved using the ideas outlined in Ref. [36]. Specifically, generalized unitarity cuts in four dimensions were used to project onto subsets of the differential equations. This typically leads to an answer close to the canonical form, where unwanted terms e.g. due to integrals vanishing on the cuts can be easily removed algorithmically, see e.g. Refs. [41, 42]. A canonical basis for very similar integrals was found in Ref. [41], and using the results from that paper the present basis choice was rather straightforward.

The one-form $d\tilde{A}$ characterizes the type of iterated integrals that are needed. In particular, given the definition $d\tilde{A} = \sum_{i=1}^{12} \mathbb{S}_i d\log(\alpha_i)$, the individual α_i are called the letters, and iterated integrals correspond to words in those letters. The set $\{\alpha_i\}$ is called alphabet.

For the specific one-form $d\tilde{A}$, the system in Eq. (3.6) can be solved in terms of a subset of generalized (or Goncharov) polylogarithms (GPL) [51, 52, 53], defined as iterated integrations over a set of basic polynomials $\{(x - a_1), \dots, (x - a_n)\}$,

$$G(0_n, x) = \frac{1}{n!} \log^n x, \quad G(a_1, a_2, \dots, a_n, x) = \int_0^x \frac{dt}{t - a_1} G(a_2, \dots, a_n, t), \quad (3.40)$$

for a certain set of a_i .

We choose to represent the GPLs of two variables, x_q and y_q , as functions of argument x_q and weights depending on y_q . The weights for the GPLs functions of x_q are determined by the following set,

$$\left\{ x_q, 1 - x_q, 1 + x_q, x_y - y_q, x_y - 1/y_q, x_q - R_i \right\}, \quad (3.41)$$

where the roots R_i are defined by the following expressions,

$$R_{01} = \frac{y_q}{y_q^2 - y_q + 1}, \quad (3.42)$$

$$R_{02} = \frac{y_q^2 - y_q + 1}{y_q}, \quad (3.43)$$

$$R_{11} = \frac{1}{2} + \frac{1}{2y_q} - \frac{1}{2y_q} \sqrt{1 + 2y_q - 3y_q^2}, \quad (3.44)$$

$$R_{12} = \frac{1}{2} + \frac{1}{2y_q} + \frac{1}{2y_q} \sqrt{1 + 2y_q - 3y_q^2}, \quad (3.45)$$

$$R_{21} = \frac{1}{2} + \frac{1}{2}y_q - \frac{1}{2} \sqrt{-3 + 2y_q + y_q^2}, \quad (3.46)$$

$$R_{22} = \frac{1}{2} + \frac{1}{2}y_q + \frac{1}{2} \sqrt{-3 + 2y_q + y_q^2}. \quad (3.47)$$

We also have GPLs of the variable y_q . The weights of these GPLs are determined by the following set,

$$\left\{ y_q, 1 - y_q, 1 + y_q, y_q - c, y_q - \bar{c}, y_q - i, y_q + i \right\}, \quad (3.48)$$

where

$$c = \frac{1 - i\sqrt{3}}{2}, \quad \bar{c} = \frac{1 + i\sqrt{3}}{2}, \quad (3.49)$$

are sixth roots of the unity.

The solution of the differential equations can be found expanding each of the canonical master integrals in ϵ ,

$$f_i = f_i^{(0)} + f_i^{(1)}\epsilon + f_i^{(2)}\epsilon^2 + \dots \quad (3.50)$$

We can identify the terms on each side of Eq. (3.6) which multiply the same power of ϵ , i.e.

$$df_i^{(k)} = d\tilde{A}_{ij} f_j^{(k-1)}. \quad (3.51)$$

This allows us to solve Eq. (3.6) recursively order by order. As the values of $f_i^{(0)}$ are constants given entirely by the boundary conditions, we shall start by finding $f_i^{(1)}(x_q, y_q)$. This may be done by integrating the right-hand side of Eq. (3.51) from the boundary point $(1, 1)$ to a general point (x_q, y_q) , and we choose to use a stepwise path passing through $(x_q, 1)$. Using the boundary conditions to fix the integration constant, gives the values for $f_i^{(1)}$. Once this is done for each of the canonical master integrals, the procedure may be repeated for $f_i^{(2)}$ and the other orders, yielding the full result for f_i up to any desired order.

We checked all the expressions of the master integrals numerically against the computer program Fiesta [54, 55, 56] finding complete agreement.

The analytic expressions of the functions f_i are collected in an ancillary file of the arXiv submission of the present paper.

A comment is due regarding analytic continuation and analytic boundary values in different regions. In the following subsections, we explain how we obtained a formula valid in all kinematic regions. For completeness, here we wish to comment that another possibility is to solve the differential equations directly starting from a boundary value in the region of interest. The boundary value we gave in Eq. (3.39) at $x_q = y_q = 1$ is in a non-physical region, and other regions can be reached by analytic continuation. In particular, when analytically continuing to negative values of x_q or y_q , the $d \log x_q$ and

$d \log y_q$ terms in $d\tilde{A}$ are responsible for imaginary parts. As an example, let us analyze the boundary point $(x_q, y_q) = (-1, -1)$. Unlike $(x_q, y_q) = (1, 1)$, this is a singular point, so that it has to be approached with care. Since $x_q = y_q$ is nonsingular, we can set $x_q = y_q = z$, for $z > 0$ in which case the alphabet becomes $\{d \log z, d \log(1 - z), d \log(1 + z)\}$. When analytically continuing to negative values of z , we have to take care of the imaginary parts due to $d \log z$, keeping in mind that z has a small imaginary part $i0$. In this way, one can give an analytic boundary value as $z \rightarrow -1$, in terms of powers of $\log(1 + z)$ and a set of constants. It follows from the reduced alphabet $\{d \log z, d \log(1 - z), d \log(1 + z)\}$ that the only constants required are Euler sums. Up to weight four, one has $i\pi, \log 2, \zeta_3, \text{Li}_4(1/2)$, and products thereof.

3.2 An alternative choice of the functional basis

The analytic expressions of the master integrals in terms of GPLs provide all the necessary features of an analytic formula: possibility to expand the formulae in particular regions of the phase space, flexibility with respect to the input physical parameters, available routines for their numerical evaluation [57]. However, for the sake of a faster and more stable numerical evaluation, we describe in this section how to represent the result in terms of a different functional basis.

Up to weight four, Goncharov polylogarithms can be rewritten in terms of the following functions (see [58] and references therein),

$$\log(x_1) = G(0, x_1), \quad \text{Li}_n(x_1) = -G(0_{n-1}, 1, x_1), \quad \text{Li}_{2,2}(x_1, x_2) = G\left(0, \frac{1}{x_2}, 0, \frac{1}{x_1 x_2}, 1\right), \quad (3.52)$$

with $n = (2, 3, 4)$, and where x_1 and x_2 are rational functions of x_q and y_q . $\text{Li}_n(x_1)$ has a branch cut for $x_1 > 1$, while $\text{Li}_{2,2}(x_1, x_2)$ has a branch cut whenever $x_1 > 1$ or $x_1 x_2 > 1$. With this choice, the functions given in Eq. (3.52) can be directly evaluated using the numerical routines of [57].

In order to find an expression in terms of these functions, the concept of the symbol [51, 59, 58] of an iterated integral is very useful. The symbol corresponds to the integration kernels defining the iterated integrals. It is completely manifest in our differential equations approach. It is possible to use symbol-based ideas to rewrite the master integrals in terms of a minimal function basis, see e.g. [60]. Moreover, we can recover the information about the terms in the kernel of the symbol using the coproduct map [61].

However, it is also possible to proceed in a more direct way, using the knowledge of the differential equations, proceeding in the following algorithmic steps. First, one generates a list of function arguments as monomials in the letters appearing in our function alphabet (i.e. the arguments of the logarithms appearing in the one-form $d\tilde{A}$.) For the classical polylogarithms $\text{Li}_n(x_1)$, one requires that $1 - x_1$ factorizes over the letters appearing in the alphabet. (A caveat is that in principle, “spurious” letters might be needed [60], but this was not the case here.) For $\text{Li}_{2,2}(x_1, x_2)$, the condition is that $1 - x_1, 1 - x_2, 1 - x_1 x_2$ factorize over the alphabet. Second, for each weight k , one chooses a maximal set of linearly independent functions for the alphabet (the linear independence can be verified using the

symbol). By construction, the differential equation at order ϵ^k can then be solved in terms of this set of functions.

The Li expressions for the master integrals are provided in an ancillary file and are defined for the relevant physical region $s > m_z^2$, which in terms of the new variables implies $y < x$ or $\arg(y) < \arg(x)$, where $0 < \arg(x) \leq \pi$ is understood.

When solving the differential equations in terms of the above functions, there is a certain freedom in the choice of the set of function arguments. The choice is usually guided by trying to make certain properties of the answer manifest, such as simple branch cut properties. For instance, one could require that the functions are real valued in the physical region, so that the imaginary parts of the master integrals become explicit. We found that this was possible in the regions of real x_q, y_q . However, for x_q or y_q complex, individual functions develop imaginary parts.

In order to obtain an expression valid over the entire physical domain, a linear combination with rational coefficients of the Li functions is not sufficient. The reason is that some of the functions in Eq. (3.52) have discontinuities in the physical region, and in order to ensure the analyticity of the master integrals it is necessary to introduce discontinuous functions (Heaviside theta functions) that cancel branch cut discontinuities of the new basis. The same issue was discussed in Ref. [60]. In Appendix D we briefly introduce the issue, and we provide a method to find an expression for the master integrals in terms of Li functions valid over the entire physical region.

4. Numerical Results

In order to assess the impact of the NLO QCD corrections, it is convenient to recall the relative contributions of the top, bottom and electroweak loops to the leading order width. For $m_H = 125.1$ GeV, $m_t = 173.34$ GeV, $m_b = 4.6$ GeV, $m_W = 80.398$ GeV, $m_Z = 91.1876$ GeV, $s_W^2 = 0.23149$, $\alpha = 1/128$, $G_F = 1.16637 \cdot 10^{-5}$, the QCD width is 0.02 KeV at leading order. In Table 1, we report the relative contributions of the top–quark loop, the bottom–quark loop and the top–bottom interference to the leading order QCD width. We note that the bottom loop contributes only one per mille to the QCD width, which is almost entirely given by the top loop, with a sizeable destructive top–bottom interference. On the other hand, the full width is 6.67 KeV at leading order. In Table 2, we report the relative contributions of the QCD (*i.e.* top and bottom) loops, the W -boson loop, and the QCD– W -boson interference to the leading–order width. We see that the QCD loops contribute only three per mille to the width at leading order; the W -boson loop accounts for the bulk of the width, up to a large destructive QCD– W -boson interference.

The NLO QCD corrections to the decay width of a Higgs boson into a Z boson and a photon were computed numerically in Ref. [14] and turn out to be quite mild. In Fig. 5, we plot the decay width as a function of the Higgs mass. $\Gamma_{H \rightarrow Z\gamma}$ includes the NLO contributions of the diagrams with a top-quark loop and a bottom-quark loop. In Fig. 6, we plot the two-loop QCD corrections to the decay width. In particular, we plot the contribution of the top loop alone, the bottom loop alone, and the complete correction.

$\Gamma_{QCD}^{(1l)}$ (KeV)	$\Gamma_t^{(1l)}/\Gamma_{QCD}^{(1l)}$	$\Gamma_b^{(1l)}/\Gamma_{QCD}^{(1l)}$	$\text{Interf}_{t-b}^{(1l)}/\Gamma_{QCD}^{(1l)}$
0.02	1.052	$1 \cdot 10^{-3}$	- 0.053

Table 1: Values of the QCD leading-order width, and of the relative contributions of the top loop, the bottom loop and of the interference between top and bottom loops, at $m_H = 125.1$ GeV.

$\Gamma^{(1l)}$ (KeV)	$\Gamma_{QCD}^{(1l)}/\Gamma^{(1l)}$	$\Gamma_W^{(1l)}/\Gamma^{(1l)}$	$\text{Interf}_{QCD-W}^{(1l)}/\Gamma^{(1l)}$
6.67	$3 \cdot 10^{-3}$	1.112	- 0.115

Table 2: Values of the leading-order width, and of the relative contributions of the QCD loops, the W -boson loop and of the interference between the QCD and the W -boson loops, at $m_H = 125.1$ GeV.

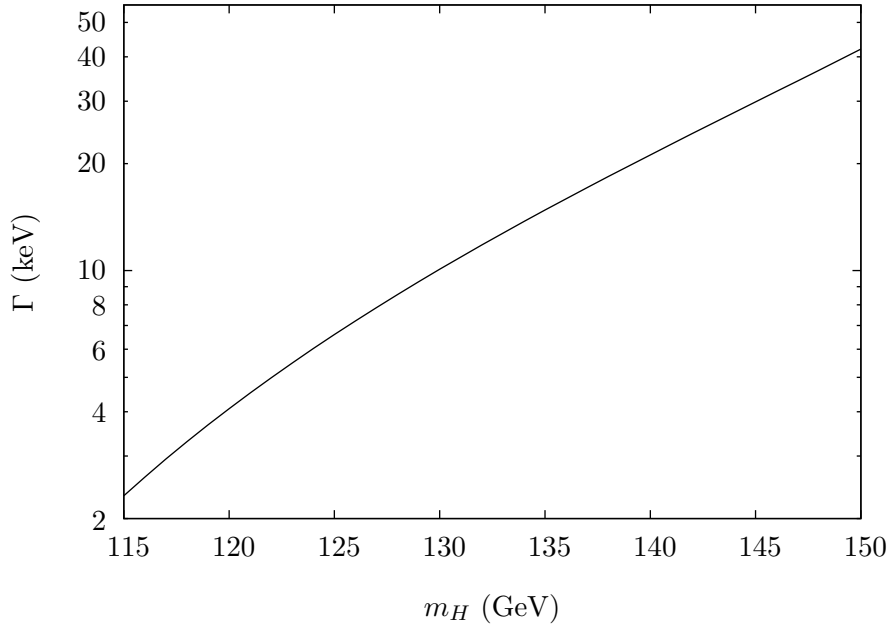


Figure 5: $\Gamma_{H \rightarrow Z\gamma}$ including LO and NLO QCD contributions.

For small values of the Higgs mass, the corrections due to the top loop and those due to the bottom have opposite sign, with the top correction being dominant. In Table 3, we quote the figures for $m_H = 125.1$ GeV and $\alpha_S(m_H^2) = 0.115$: the two-loop QCD corrections amount to 0.22% of the leading order width, with the top loop adding a 0.3% and the bottom loop subtracting a 0.08%. The two-loop top corrections is in agreement with the corresponding plot of Ref. [14] and with the results in Ref. [62]

As we recalled above, at one loop the top and bottom loops contribute 0.3% of the leading order width. Since the two-loop QCD contribution is about 75% of the one-loop QCD contribution, that implies a bad convergence of the QCD part of the width. In principle, higher QCD orders would be necessary to stabilise the QCD perturbative series.

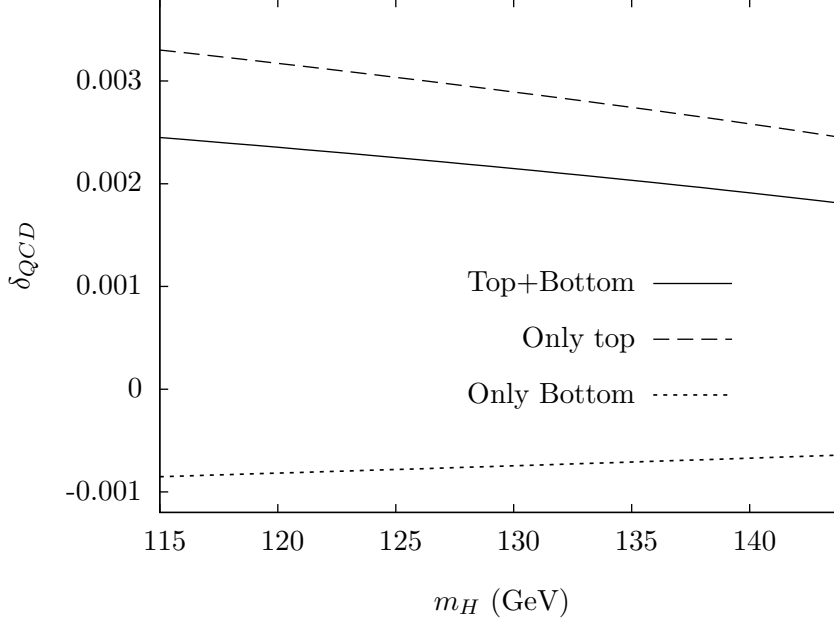


Figure 6: The size of the NLO QCD corrections with respect to the leading order contribution, δ_{QCD} , as defined in Eq. (3.5). In this figure we plot the contribution of the top loop only, the bottom loop only, and the top and bottom loops.

Γ (KeV)	δ_{QCD} (top)	δ_{QCD} (bottom)	δ_{QCD}
6.68	$3 \cdot 10^{-3}$	$-0.8 \cdot 10^{-3}$	$2.2 \cdot 10^{-3}$

Table 3: Values of the NLO QCD width, and of the NLO QCD corrections δ_{QCD} with respect to the leading order contribution, at $m_H = 125.1$ GeV.

However, up to NLO accuracy, the QCD contribution is numerically tiny. Thus, it would be more relevant to compute the two-loop electroweak corrections, which we expect to be larger than the QCD ones.

5. Conclusions

In this paper we present the analytic calculation of the NLO QCD corrections to the width of a Higgs boson decaying to a Z boson and a photon. These corrections were computed numerically in [14], where the authors studied the size of the corrections that come from the two-loop Feynman diagrams with a top-quark loop, with respect to the leading order contribution. In our paper we include also the contribution due to the two-loop diagrams with a bottom-quark loop. For small values of the Higgs mass, the corrections due to the top loop and those due to the bottom have opposite sign, with the top correction being dominant. For $m_H = 125.1$ GeV they amount to 0.22% of the leading order width.

The calculation was carried out using integration-by-parts identities for the reduction to master integrals of the dimensionally regularized scalar integrals, in terms of which we

expressed the amplitude. The calculation of the master integrals was performed using the Differential Equations Method applied to a set of functions suitably chosen to be of uniform weight.

The solution is expressed in terms of logarithms and polylogarithmic functions Li_n , with $n = 2, 3, 4$, and $\text{Li}_{2,2}$. Their arguments are rational expressions in the two dimensionless variables x_q, y_q , written in terms of the three mass scales of the problem: m_H, m_Z and m_q . The numerical evaluation of the polylogarithmic functions is done using existing numerical C++ routines.

Finally, we recall that for $m_H = 125.1$ GeV, at leading order the top and the bottom loops account for about 0.3% of the width, the overwhelming contribution being yielded by the electroweak loop. Having found that the two-loop QCD corrections, which correct the heavy-quark loop, equal about 0.22% of the leading order width, it is reasonable to expect that the two-loop electroweak corrections, which correct the electroweak loop, will yield a larger contribution [‡].

Acknowledgments

We are grateful to D. Kara for providing the results of their independent calculation for a detailed comparison before the publication [62]. Some of the algebraic manipulations required in this work were carried out with FORM [68]. The Feynman diagrams were generated by FeynArts [69, 70] and drawn with Axodraw [71]. The work of VS was partially supported by the Alexander von Humboldt Foundation (Humboldt Forschungspreis). The work of RB was partly supported by European Community Seventh Framework Programme FP7/2007-2013, under grant agreement N.302997. The work of JMH was supported in part by the DOE grant DE-SC0009988, and by the Marvin L. Goldberger fund. The work of VDD, HF, JMH and VS was partly supported by the Research Executive Agency (REA) of the European Union, through the Initial Training Network LHCPHenoNet under contract PITN-GA-2010-264564. The work of HF is supported in part by the European Commission through the HiggsTools Initial Training Network PITN-GA-2012-316704. RB, VDD and FM would like to thank the Galileo Galilei Institute for Theoretical Physics for hospitality during the completion of this work.

[‡]The Z boson may decay leptonically – the final state of $H \rightarrow Z\gamma$ is a lepton pair, l^-l^+ , and a photon – or hadronically – the final state is formed by two jets and a photon. However, the two-jet plus photon final state is overwhelmed by the QCD background. Conversely, because of the smaller $pp \rightarrow l^-l^+\gamma$ background, the decay $H \rightarrow Z\gamma \rightarrow l^-l^+\gamma$ is much cleaner. In order to compare to the $pp \rightarrow l^-l^+\gamma$ background, it is different to consider the resonant production $H \rightarrow Z\gamma \rightarrow l^-l^+\gamma$ or the off-resonant one $H \rightarrow l^-l^+\gamma$, for which no on-shell Z -boson is produced in the intermediate state. Estimates of the difference between the resonant and the off-resonant widths vary [63, 64, 65, 66], however with realistic experimental cuts, the difference between the resonant and off-resonant leading-order widths for electron or muon pairs is of the order of a few per cent [67]. As regards the two-loop QCD corrections we computed, the off-resonant diagrams are not present. Thus, with little effort – just including the Z -boson decay into two leptons – we could have obtained the QCD corrections to the decay $H \rightarrow l^-l^+\gamma$. However, as regards the two-loop electroweak corrections, there are also off-resonant diagrams. Therefore, expecting that the still unknown two-loop electroweak corrections may be larger than the two-loop QCD corrections, we think it is best to postpone an analysis of the $H \rightarrow l^-l^+\gamma$ decay to the computation of the two-loop electroweak corrections.

A. Projection operators

The projector operators to be used in Eq. (2.2) are

$$P_1^{\mu\nu} = \frac{4}{(m_H^2 - m_Z^2)^2} p_2^\mu p_2^\nu \quad (\text{A.1})$$

$$P_2^{\mu\nu} = \frac{4}{(m_H^2 - m_Z^2)^2} p_1^\mu p_1^\nu + \frac{16(d-1)m_Z^4}{(d-2)(m_H^2 - m_Z^2)^4} p_2^\mu p_2^\nu - \frac{8(d-1)m_Z^2}{(d-2)(m_H^2 - m_Z^2)^3} [p_1^\mu p_2^\nu + p_2^\mu p_1^\nu] - \frac{4m_Z^2}{(d-2)(m_H^2 - m_Z^2)^2} \delta^{\mu\nu}, \quad (\text{A.2})$$

$$P_3^{\mu\nu} = -\frac{8(d-1)m_Z^2}{(d-2)(m_H^2 - m_Z^2)^3} p_2^\mu p_2^\nu + \frac{4}{(d-2)(m_H^2 - m_Z^2)^2} p_1^\mu p_2^\nu + \frac{4(d-1)}{(d-2)(m_H^2 - m_Z^2)^2} p_2^\mu p_1^\nu + \frac{2}{(d-2)(m_H^2 - m_Z^2)} \delta^{\mu\nu}, \quad (\text{A.3})$$

$$P_4^{\mu\nu} = -\frac{8(d-1)m_Z^2}{(d-2)(m_H^2 - m_Z^2)^3} p_2^\mu p_2^\nu + \frac{4(d-1)}{(d-2)(m_H^2 - m_Z^2)^2} p_1^\mu p_2^\nu + \frac{4}{(d-2)(m_H^2 - m_Z^2)^2} p_2^\mu p_1^\nu + \frac{2}{(d-2)(m_H^2 - m_Z^2)} \delta^{\mu\nu}, \quad (\text{A.4})$$

$$P_5^{\mu\nu} = -\frac{4m_Z^2}{(d-2)(m_H^2 - m_Z^2)^2} p_2^\mu p_2^\nu + \frac{2}{(d-2)(m_H^2 - m_Z^2)} [p_1^\mu p_2^\nu + p_2^\mu p_1^\nu] + \frac{1}{(d-2)} \delta^{\mu\nu}, \quad (\text{A.5})$$

$$P_6^{\mu\nu} = -\frac{4}{(d-2)(d-3)(m_H^2 - m_Z^2)^2} \epsilon^{\mu\nu\rho\sigma} p_{1\rho} p_{2\sigma}. \quad (\text{A.6})$$

B. Primary master integrals

In this appendix we give the explicit expression of the “primary” master integrals shown in Fig. 4.

We define the following set of seven denominators,

$$D_1 = k_1^2 + m_q^2, \quad (\text{B.1})$$

$$D_2 = k_2^2, \quad (\text{B.2})$$

$$D_3 = (k_1 + k_2)^2 + m_q^2, \quad (\text{B.3})$$

$$D_4 = (p_1 - k_1)^2 + m_q^2, \quad (\text{B.4})$$

$$D_5 = (p_2 + k_1)^2 + m_q^2, \quad (\text{B.5})$$

$$D_6 = (p_1 - k_1 - k_2)^2 + m_q^2, \quad (\text{B.6})$$

$$D_7 = (p_2 + k_1 + k_2)^2 + m_q^2. \quad (\text{B.7})$$

The integrals of Fig. 4 are then,

$$M_1 = \int \mathcal{D}^D k_1 \mathcal{D}^D k_2 \frac{1}{D_1^2 D_3^2}, \quad M_2 = \int \mathcal{D}^D k_1 \mathcal{D}^D k_2 \frac{1}{D_3^2 D_4^2 D_5^2}, \quad (\text{B.8})$$

$$M_3 = \int \mathcal{D}^D k_1 \mathcal{D}^D k_2 \frac{1}{D_1^2 D_3^2 D_4}, \quad M_4 = \int \mathcal{D}^D k_1 \mathcal{D}^D k_2 \frac{1}{D_2 D_5^2 D_6^2}, \quad (\text{B.9})$$

$$M_5 = \int \mathcal{D}^D k_1 \mathcal{D}^D k_2 \frac{1}{D_2 D_3^2 D_4^2}, \quad M_6 = \int \mathcal{D}^D k_1 \mathcal{D}^D k_2 \frac{1}{D_2^2 D_5^2 D_6}, \quad (\text{B.10})$$

$$M_7 = \int \mathcal{D}^D k_1 \mathcal{D}^D k_2 \frac{1}{D_2^2 D_3^2 D_4}, \quad M_8 = \int \mathcal{D}^D k_1 \mathcal{D}^D k_2 \frac{1}{D_1 D_3^2 D_4 D_5}, \quad (\text{B.11})$$

$$M_9 = \int \mathcal{D}^D k_1 \mathcal{D}^D k_2 \frac{1}{D_4^2 D_5 D_6^2 D_7}, \quad M_{10} = \int \mathcal{D}^D k_1 \mathcal{D}^D k_2 \frac{1}{D_1^2 D_3^2 D_4 D_6}, \quad (\text{B.12})$$

$$M_{11} = \int \mathcal{D}^D k_1 \mathcal{D}^D k_2 \frac{1}{D_3^2 D_4^2 D_5 D_6}, \quad M_{12} = \int \mathcal{D}^D k_1 \mathcal{D}^D k_2 \frac{1}{D_1 D_2 D_5 D_6^2}, \quad (\text{B.13})$$

$$M_{13} = \int \mathcal{D}^D k_1 \mathcal{D}^D k_2 \frac{1}{D_2 D_3^2 D_4 D_5}, \quad M_{14} = \int \mathcal{D}^D k_1 \mathcal{D}^D k_2 \frac{1}{D_2 D_3^3 D_4 D_5}, \quad (\text{B.14})$$

$$M_{15} = \int \mathcal{D}^D k_1 \mathcal{D}^D k_2 \frac{k_1^2 + m_q^2}{D_2 D_3^2 D_4^2 D_5}, \quad M_{16} = \int \mathcal{D}^D k_1 \mathcal{D}^D k_2 \frac{1}{D_2 D_3 D_5^2 D_6}, \quad (\text{B.15})$$

$$M_{17} = \int \mathcal{D}^D k_1 \mathcal{D}^D k_2 \frac{1}{D_2 D_3 D_5^3 D_6}, \quad M_{18} = \int \mathcal{D}^D k_1 \mathcal{D}^D k_2 \frac{(p_2 + k_1 + k_2)^2}{D_2 D_3^2 D_5^2 D_6}, \quad (\text{B.16})$$

$$M_{19} = \int \mathcal{D}^D k_1 \mathcal{D}^D k_2 \frac{1}{D_1 D_4 D_5 D_6^2 D_7}, \quad M_{20} = \int \mathcal{D}^D k_1 \mathcal{D}^D k_2 \frac{1}{D_1 D_3^2 D_4 D_5 D_6}, \quad (\text{B.17})$$

$$M_{21} = \int \mathcal{D}^D k_1 \mathcal{D}^D k_2 \frac{1}{D_1 D_2 D_3 D_5 D_6}, \quad M_{22} = \int \mathcal{D}^D k_1 \mathcal{D}^D k_2 \frac{1}{D_1 D_2 D_3 D_5 D_6^2}, \quad (\text{B.18})$$

$$M_{23} = \int \mathcal{D}^D k_1 \mathcal{D}^D k_2 \frac{1}{D_2 D_3 D_4 D_5 D_7}, \quad M_{24} = \int \mathcal{D}^D k_1 \mathcal{D}^D k_2 \frac{1}{D_2 D_3 D_4^2 D_5 D_7}, \quad (\text{B.19})$$

$$M_{25} = \int \mathcal{D}^D k_1 \mathcal{D}^D k_2 \frac{1}{D_2 D_3 D_4 D_5 D_6}, \quad M_{26} = \int \mathcal{D}^D k_1 \mathcal{D}^D k_2 \frac{1}{D_2 D_3^2 D_4 D_5 D_6}, \quad (\text{B.20})$$

$$M_{27} = \int \mathcal{D}^D k_1 \mathcal{D}^D k_2 \frac{1}{D_2 D_3 D_4 D_5^2 D_6}, \quad M_{28} = \int \mathcal{D}^D k_1 \mathcal{D}^D k_2 \frac{1}{D_2 D_3^2 D_4 D_5^2 D_6}. \quad (\text{B.21})$$

C. Matrices for the System of Differential Equations

In this appendix we collect the matrices \mathbb{S}_1 – \mathbb{S}_{12} defined in Eq. (3.38).

$$S_1 =$$

$$S_2 =$$

$$S_3 =$$

$$S_4 =$$

$$S_5 =$$

$$S_6 =$$

$$S_7 =$$

$$S_8 =$$

$$S_9 =$$

$$S_{10} =$$

$$S_{11} =$$

$$S_{12} =$$

D. Solution of the differential equations in terms of Li functions

By definition the solution of the differential equations can be valid only in a region where the differential equations are non-singular. When a singular point of the differential equations is reached the solution might develop a branch cut, depending on the functional basis used to represent the solution. However in a physical process the master integrals are analytic in the physical region and those branch cuts must be spurious. In order to ensure the right analytic properties of the master integrals, we can replace the discontinuous functions with different, analytic branches.

Solving the differential equations in terms of Li functions, we can in principle find a basis without branch cuts in the physical region, so that the solution has the right analytic structure and no spurious branch cuts are present. However in our case the set of analytic functions in the physical region is too small to represent the master integrals, and we are forced to employ also discontinuous functions. For simplicity they are chosen to be the following two logarithms and five Li_3 ,

$$\log(x_q - y_q), \log(-y_q x_q^2 + y_q x_q - y_q + x_q), \text{Li}_3(a_i) \ i = 1, \dots, 5. \quad (\text{D.1})$$

where the a_i 's are

$$\vec{a} = \left\{ \frac{x_q y_q^2 - x_q y_q + x_q - y_q}{(x_q + 1)(1 - y_q)^2}, \frac{-x_q y_q^2 + x_q y_q - x_q + y_q}{(1 - x_q)(x_q + 1)y_q}, \frac{-x_q y_q^2 + x_q y_q - x_q + y_q}{(x_q + 1)(y_q - x_q)(1 - x_q y_q)}, \right. \\ \left. \frac{x_q y_q^2 - x_q y_q + x_q - y_q}{x_q y_q - y_q^2 + y_q - 1}, \frac{x_q y_q^2 - x_q y_q + x_q - y_q}{x_q (-x_q y_q + y_q^2 - y_q + 1)} \right\}. \quad (\text{D.2})$$

Let us show how to find the analytic branch of $\log(x_q - y_q)$ in the physical region. The values of the argument cover a region in the second, third and fourth quadrant of the complex plane, positive real axis included, intersecting the cut of the logarithm. An analytic branch can be found, for every polylogarithm, subtracting the discontinuity of the function across the branch cut. In the present case $\text{Disc}(\log(x)) = 2\pi i$ so that the analytic branch, $\log^*(x)$, is

$$\log^*(x_q - y_q) = \log(x_q - y_q) - 2i\pi \theta(\Im(x_q - y_q)), \quad (\text{D.3})$$

where $\theta(x)$ is the Heaviside θ function. Note that employing θ functions we introduce a (removable) discontinuity on the real axis. In the next section we show how to remove this discontinuity.

For $\text{Li}_3(a_i)$ the a_i 's lie on the branch cut whenever $\Re(a_i) > 1$. We remove the cut ambiguity recalling that the physical region is defined via the Feynman prescription, and in order to get an analytic function we use the analytic continuation of Li_3 whenever $\Re(a_i) > 1$. This can be achieved, again, by means of θ functions,

$$\text{Li}_3^*(a_i) = \theta(1 - \Re(a_i))\text{Li}_3(a_i) + \theta(\Re(a_i) - 1)\text{C}_3(a_i, \sigma_i), \quad (\text{D.4})$$

where σ_i is the sign of the imaginary part of a_i due to Feynman prescription,

$$\vec{\sigma} = \{-1, -1, -1, 1, 1\}, \quad (\text{D.5})$$

and C_3 is the analytic continuation of Li_3 ,

$$C_3(a_i, \sigma_i) = \text{Li}_3\left(\frac{1}{a_i}\right) - \frac{1}{6} \log^3(a_i) + \sigma_i \frac{1}{2} i\pi \log^2(a_i) + \frac{1}{3} \pi^2 \log(a_i). \quad (\text{D.6})$$

D.1 Analytic branches in the physical region

The representations (D.3) and (D.4) are analytic everywhere in the physical region, but if the argument of the θ function is zero the expression is not defined. Nevertheless, by construction, the new basis has no branch cuts and the limits to the discontinuous points are well defined. In order to remove these (spurious) discontinuities we impose the limiting values as long as the arguments of the θ functions vanish.

The limiting values to the real axis of Eq. (D.3) are such that $\log^*(-1) = -i\pi$ and $\log^*(x > 0)$ is positive. This uniquely defines Eq. (D.3) over the entire physical region. With a similar reasoning we can find the analytic branch, $\log^\dagger(x)$, of the second logarithm of Eq. (D.1). Defining $a = x_q - y_q$ and $b = -y_q x_q^2 + y_q x_q - y_q + x_q$ we arrive at

$$\begin{aligned} \log^*(a) &= [1 - \delta(\Im(a))] c(a) + \delta(\Im(a)) [\Re(\log(a)) - i\pi], \\ \log^\dagger(b) &= [1 - \delta(\Im(b))] d(b) + \delta(\Im(b)) [\Re(\log(b)) - i\pi(1 + \theta_{1/2}(x_q, y_q))], \end{aligned} \quad (\text{D.7})$$

where

$$\delta(x) = \begin{cases} 1 & \text{for } x = 0 \\ 0 & \text{otherwise} \end{cases}, \quad (\text{D.8})$$

and

$$\begin{aligned} c(a) &= \log(a) - 2i\pi \theta(\Im(a)), \\ d(b) &= \log(b) - 2i\pi \theta(\Im(b)) - 2i\pi \theta_{1/2}(x_q, y_q) \theta(-\Im(b)), \\ \theta_{1/2}(x_q, y_q) &= \theta_0(\pi/2 - \arg(x_q)) \theta_0(\pi/2 - \arg(y_q)), \end{aligned} \quad (\text{D.9})$$

where $0 < \arg(x) \leq \pi$.

In Eq. (D.4), $\text{Li}_3(1) = C_3(1, \sigma_i)$, then

$$\text{Li}_3^*(a_i) = \theta_0(1 - \Re(a_i)) \text{Li}_3(a_i) + \theta_1(\Re(a_i) - 1) C_3(a_i, \sigma_i), \quad (\text{D.10})$$

where $\theta_0(x)$ and $\theta_1(x)$ are modified Heaviside θ functions, such that $\theta_0(0) = 0$ and $\theta_1(0) = 1$.

Note that Eqs. (D.7) do not hold if x_q, y_q are both real, where the standard \log has to be used. To avoid clutter we omit here the extra terms extending the validity of Eq. (D.7) to that region, while they are present in the ancillary files of the arXiv submission. Although the above representations might look cumbersome, they are nothing but simple combinations of elementary functions like the Heaviside θ , and implementing them for numeric evaluations is straightforward computer algebra. The expressions in the ancillary files make only use of built-in **Mathematica** functions.

References

- [1] **ATLAS** Collaboration, G. Aad et al., *Observation of a new particle in the search for the Standard Model Higgs boson with the ATLAS detector at the LHC*, *Phys.Lett.* **B716** (2012) 1–29, [[arXiv:1207.7214](#)].
- [2] **CMS** Collaboration, S. Chatrchyan et al., *Observation of a new boson at a mass of 125 GeV with the CMS experiment at the LHC*, *Phys.Lett.* **B716** (2012) 30–61, [[arXiv:1207.7235](#)].
- [3] **LHC Higgs Cross Section Working Group** Collaboration, S. Heinemeyer et al., *Handbook of LHC Higgs Cross Sections: 3. Higgs Properties*, [arXiv:1307.1347](#).
- [4] **CMS** Collaboration, S. Chatrchyan et al., *Search for a Higgs boson decaying into a Z and a photon in pp collisions at $\sqrt{s} = 7$ and 8 TeV*, *Phys.Lett.* **B726** (2013) 587–609, [[arXiv:1307.5515](#)].
- [5] **ATLAS** Collaboration, G. Aad et al., *Search for Higgs boson decays to a photon and a Z boson in pp collisions at $\sqrt{s}=7$ and 8 TeV with the ATLAS detector*, *Phys.Lett.* **B732** (2014) 8–27, [[arXiv:1402.3051](#)].
- [6] R. Cahn, M. S. Chanowitz, and N. Fleishon, *Higgs Particle Production by Z to H Gamma*, *Phys.Lett.* **B82** (1979) 113.
- [7] L. Bergstrom and G. Hulth, *Induced Higgs Couplings to Neutral Bosons in e^+e^- Collisions*, *Nucl.Phys.* **B259** (1985) 137.
- [8] I. Low, J. Lykken, and G. Shaughnessy, *Singlet scalars as Higgs imposters at the Large Hadron Collider*, *Phys.Rev.* **D84** (2011) 035027, [[arXiv:1105.4587](#)].
- [9] I. Low, J. Lykken, and G. Shaughnessy, *Have We Observed the Higgs (Imposter)?*, *Phys.Rev.* **D86** (2012) 093012, [[arXiv:1207.1093](#)].
- [10] A. Azatov, R. Contino, A. Di Iura, and J. Galloway, *New Prospects for Higgs Compositeness in $h \rightarrow Z\gamma$* , *Phys.Rev.* **D88** (2013), no. 7 075019, [[arXiv:1308.2676](#)].
- [11] M. Carena, I. Low, and C. E. Wagner, *Implications of a Modified Higgs to Diphoton Decay Width*, *JHEP* **1208** (2012) 060, [[arXiv:1206.1082](#)].
- [12] C.-W. Chiang and K. Yagyu, *Higgs boson decays to $\gamma\gamma$ and $Z\gamma$ in models with Higgs extensions*, *Phys.Rev.* **D87** (2013), no. 3 033003, [[arXiv:1207.1065](#)].
- [13] C.-S. Chen, C.-Q. Geng, D. Huang, and L.-H. Tsai, *New Scalar Contributions to $h \rightarrow Z\gamma$* , *Phys.Rev.* **D87** (2013) 075019, [[arXiv:1301.4694](#)].
- [14] M. Spira, A. Djouadi, and P. Zerwas, *QCD corrections to the H Z gamma coupling*, *Phys.Lett.* **B276** (1992) 350–353.
- [15] W. A. Bardeen, A. Buras, D. Duke, and T. Muta, *Deep Inelastic Scattering Beyond the Leading Order in Asymptotically Free Gauge Theories*, *Phys.Rev.* **D18** (1978) 3998.
- [16] G. 't Hooft and M. Veltman, *Regularization and Renormalization of Gauge Fields*, *Nucl.Phys.* **B44** (1972) 189–213.
- [17] C. Bollini and J. Giambiagi, *Lowest order divergent graphs in nu-dimensional space*, *Phys.Lett.* **B40** (1972) 566–568.
- [18] C. Bollini and J. Giambiagi, *Dimensional Renormalization: The Number of Dimensions as a Regularizing Parameter*, *Nuovo Cim.* **12** (1972), no. 1 20–26.

- [19] J. Ashmore, *A Method of Gauge Invariant Regularization*, *Lett.Nuovo Cim.* **4** (1972) 289–290.
- [20] G. Cicuta and E. Montaldi, *Analytic renormalization via continuous space dimension*, *Lett.Nuovo Cim.* **4** (1972) 329–332.
- [21] R. Gastmans and R. Meuldermans, *Dimensional regularization of the infrared problem*, *Nucl.Phys.* **B63** (1973) 277–284.
- [22] A. Smirnov, *Algorithm FIRE – Feynman Integral REduction*, *JHEP* **0810** (2008) 107, [[arXiv:0807.3243](#)].
- [23] A. Smirnov and V. Smirnov, *FIRE4, LiteRed and accompanying tools to solve integration by parts relations*, *Comput.Phys.Commun.* **184** (2013) 2820–2827, [[arXiv:1302.5885](#)].
- [24] A. V. Smirnov, *FIRE5: a C++ implementation of Feynman Integral REduction*, *Comput.Phys.Commun.* **189** (2014) 182–191, [[arXiv:1408.2372](#)].
- [25] C. Studerus, *Reduze-Feynman Integral Reduction in C++*, *Comput.Phys.Commun.* **181** (2010) 1293–1300, [[arXiv:0912.2546](#)].
- [26] A. von Manteuffel and C. Studerus, *Reduze 2 - Distributed Feynman Integral Reduction*, [arXiv:1201.4330](#).
- [27] F. Tkachov, *A Theorem on Analytical Calculability of Four Loop Renormalization Group Functions*, *Phys.Lett.* **B100** (1981) 65–68.
- [28] K. Chetyrkin and F. Tkachov, *Integration by Parts: The Algorithm to Calculate beta Functions in 4 Loops*, *Nucl.Phys.* **B192** (1981) 159–204.
- [29] A. Kotikov, *Differential equations method: New technique for massive Feynman diagrams calculation*, *Phys.Lett.* **B254** (1991) 158–164.
- [30] A. Kotikov, *Differential equations method: The Calculation of vertex type Feynman diagrams*, *Phys.Lett.* **B259** (1991) 314–322.
- [31] A. Kotikov, *Differential equation method: The Calculation of N point Feynman diagrams*, *Phys.Lett.* **B267** (1991) 123–127.
- [32] E. Remiddi, *Differential equations for Feynman graph amplitudes*, *Nuovo Cim.* **A110** (1997) 1435–1452, [[hep-th/9711188](#)].
- [33] M. Caffo, H. Czyz, S. Laporta, and E. Remiddi, *The Master differential equations for the two loop sunrise selfmass amplitudes*, *Nuovo Cim.* **A111** (1998) 365–389, [[hep-th/9805118](#)].
- [34] T. Gehrmann and E. Remiddi, *Differential equations for two loop four point functions*, *Nucl.Phys.* **B580** (2000) 485–518, [[hep-ph/9912329](#)].
- [35] M. Argeri and P. Mastrolia, *Feynman Diagrams and Differential Equations*, *Int.J.Mod.Phys.* **A22** (2007) 4375–4436, [[arXiv:0707.4037](#)].
- [36] J. M. Henn, *Multiloop integrals in dimensional regularization made simple*, *Phys.Rev.Lett.* **110** (2013), no. 25 251601, [[arXiv:1304.1806](#)].
- [37] J. M. Henn and V. A. Smirnov, *Analytic results for two-loop master integrals for Bhabha scattering I*, *JHEP* **1311** (2013) 041, [[arXiv:1307.4083](#)].
- [38] J. M. Henn, A. V. Smirnov, and V. A. Smirnov, *Evaluating single-scale and/or non-planar diagrams by differential equations*, *JHEP* **1403** (2014) 088, [[arXiv:1312.2588](#)].

- [39] J. M. Henn, K. Melnikov, and V. A. Smirnov, *Two-loop planar master integrals for the production of off-shell vector bosons in hadron collisions*, *JHEP* **1405** (2014) 090, [[arXiv:1402.7078](#)].
- [40] F. Caola, J. M. Henn, K. Melnikov, and V. A. Smirnov, *Non-planar master integrals for the production of two off-shell vector bosons in collisions of massless partons*, *JHEP* **1409** (2014) 043, [[arXiv:1404.5590](#)].
- [41] S. Caron-Huot and J. M. Henn, *Iterative structure of finite loop integrals*, *JHEP* **1406** (2014) 114, [[arXiv:1404.2922](#)].
- [42] T. Gehrmann, A. von Manteuffel, L. Tancredi, and E. Weihs, *The two-loop master integrals for $q\bar{q} \rightarrow VV$* , *JHEP* **1406** (2014) 032, [[arXiv:1404.4853](#)].
- [43] M. Argeri, S. Di Vita, P. Mastrolia, E. Mirabella, J. Schlenk, et al., *Magnus and Dyson Series for Master Integrals*, *JHEP* **1403** (2014) 082, [[arXiv:1401.2979](#)].
- [44] M. Hoeschele, J. Hoff, and T. Ueda, *Adequate bases of phase space master integrals for $gg \rightarrow h$ at NNLO and beyond*, *JHEP* **1409** (2014) 116, [[arXiv:1407.4049](#)].
- [45] F. Dulat and B. Mistlberger, *Real-Virtual-Virtual contributions to the inclusive Higgs cross section at N³LO*, [arXiv:1411.3586](#).
- [46] G. Bell and T. Huber, *Master integrals for the two-loop penguin contribution in non-leptonic B-decays*, *JHEP* **1412** (2014) 129, [[arXiv:1410.2804](#)].
- [47] J. M. Henn, *Lectures on differential equations for Feynman integrals*, *J.Phys.* **A48** (2015), no. 15 153001, [[arXiv:1412.2296](#)].
- [48] R. N. Lee, *Reducing differential equations for multiloop master integrals*, [arXiv:1411.0911](#).
- [49] C. Kurz, *Two-Loop QCD Corrections for the Production and Decays of Higgs Bosons*, Diploma Thesis, University of Freiburg, Germany. (December 2005).
- [50] K.-T. Chen, *Iterated path integrals*, *Bull. Amer. Math. Soc.* **83** (1977) 831–879.
- [51] A. B. Goncharov, *Multiple polylogarithms, cyclotomy and modular complexes*, *Math.Res.Lett.* **5** (1998) 497–516, [[arXiv:1105.2076](#)].
- [52] D. J. Broadhurst, *Massive three - loop Feynman diagrams reducible to SC* primitives of algebras of the sixth root of unity*, *Eur.Phys.J.* **C8** (1999) 311–333, [[hep-th/9803091](#)].
- [53] E. Remiddi and J. Vermaseren, *Harmonic polylogarithms*, *Int.J.Mod.Phys.* **A15** (2000) 725–754, [[hep-ph/9905237](#)].
- [54] A. Smirnov and M. Tentyukov, *Feynman Integral Evaluation by a Sector decomposiTiOn Approach (FIESTA)*, *Comput.Phys.Commun.* **180** (2009) 735–746, [[arXiv:0807.4129](#)].
- [55] A. Smirnov, V. Smirnov, and M. Tentyukov, *FIESTA 2: Parallelizeable multiloop numerical calculations*, *Comput.Phys.Commun.* **182** (2011) 790–803, [[arXiv:0912.0158](#)].
- [56] A. V. Smirnov, *FIESTA 3: cluster-parallelizable multiloop numerical calculations in physical regions*, *Comput.Phys.Commun.* **185** (2014) 2090–2100, [[arXiv:1312.3186](#)].
- [57] J. Vollinga and S. Weinzierl, *Numerical evaluation of multiple polylogarithms*, *Comput.Phys.Commun.* **167** (2005) 177, [[hep-ph/0410259](#)].
- [58] A. B. Goncharov, M. Spradlin, C. Vergu, and A. Volovich, *Classical Polylogarithms for Amplitudes and Wilson Loops*, *Phys.Rev.Lett.* **105** (2010) 151605, [[arXiv:1006.5703](#)].

- [59] F. C. S. Brown, *Multiple zeta values and periods of moduli spaces $\mathfrak{M}_{0,n}$* , *ArXiv Mathematics e-prints* (June, 2006) [[math/0606419](#)].
- [60] C. Duhr, H. Gangl, and J. R. Rhodes, *From polygons and symbols to polylogarithmic functions*, *JHEP* **1210** (2012) 075, [[arXiv:1110.0458](#)].
- [61] C. Duhr, *Hopf algebras, coproducts and symbols: an application to Higgs boson amplitudes*, *JHEP* **1208** (2012) 043, [[arXiv:1203.0454](#)].
- [62] T. Gehrmann, S. Guns, and D. Kara, *The rare decay $H \rightarrow Z\gamma$ in perturbative QCD*, in preparation.
- [63] L.-B. Chen, C.-F. Qiao, and R.-L. Zhu, *Reconstructing the 125 GeV SM Higgs Boson Through $\ell\bar{\ell}\gamma$* , *Phys.Lett.* **B726** (2013) 306–311, [[arXiv:1211.6058](#)].
- [64] D. A. Dicus and W. W. Repko, *Calculation of the decay $H \rightarrow e\bar{e}\gamma$* , *Phys.Rev.* **D87** (2013), no. 7 077301, [[arXiv:1302.2159](#)].
- [65] Y. Sun, H.-R. Chang, and D.-N. Gao, *Higgs decays to gamma $l+l-$ in the standard model*, *JHEP* **1305** (2013) 061, [[arXiv:1303.2230](#)].
- [66] G. Passarino, *Higgs Boson Production and Decay: Dalitz Sector*, *Phys.Lett.* **B727** (2013) 424–431, [[arXiv:1308.0422](#)].
- [67] D. A. Dicus, C. Kao, and W. W. Repko, *Comparison of $H \rightarrow \ell\bar{\ell}\gamma$ and $H \rightarrow \gamma Z, Z \rightarrow \ell\bar{\ell}$ including the ATLAS cuts*, *Phys.Rev.* **D89** (2014) 033013, [[arXiv:1310.4380](#)].
- [68] J. Kuipers, T. Ueda, J. Vermaseren, and J. Vollinga, *FORM version 4.0*, *Comput.Phys.Comm.* **184** (2013) 1453–1467, [[arXiv:1203.6543](#)].
- [69] J. Kublbeck, M. Bohm, and A. Denner, *Feyn Arts: Computer Algebraic Generation of Feynman Graphs and Amplitudes*, *Comput.Phys.Comm.* **60** (1990) 165–180.
- [70] T. Hahn, *Generating Feynman diagrams and amplitudes with FeynArts 3*, *Comput.Phys.Comm.* **140** (2001) 418–431, [[hep-ph/0012260](#)].
- [71] J. Vermaseren, *Axodraw*, *Comput.Phys.Comm.* **83** (1994) 45–58.